synapses from 13- to 23-day-old rats was 0.50 ± 0.07 (n = 3) from dual whole-cell recording and 0.39 ± 0.04 (n = 14) from focal stimulation (no significant difference, t = 1.36).
14. R. J. Sayer, M. J. Friedlander, S. J. Redman, *J. Neurosci.* **10**, 826 (1990).
15. C. Rosenmund, J. D. Clements, G. L. Westbrook, *Science* **262**, 754 (1993); N. A. Hessler, A. M. Shirker, R. Malinow, *Nature* **366**, 569 (1993).
16. B. Katz, *The Release of Neural Transmitter Substances* (Liverpool Univ. Press, Liverpool, UK, 1969).
17. F. Edwards, *Nature* **350**, 271 (1991).
18. D. M. Kullman, *Neuron* **12**, 1111 (1994).
19. R. Malinow, *Science* **266**, 1195 (1994).
20. D. Liao, N. A. Hessler, R. Malinow, *Nature* **375**, 400 (1995).
21. R. S. Zucker, *Annu. Rev. Neurosci.* **12**, 13 (1989).
22. Averaged values of quantal parameters for PPF in 1-week-old animals: First EPSC, P_r = 0.93 ± 0.03, quantal amplitude = −4.29 ± 0.18 pA, CV of quantal peak = 30.21 ± 0.48%; second EPSC, P_r = 0.21 ± 0.08 [significantly different from first EPSC (t = 6.38, $P < 0.005$; paired t test], quantal amplitude = − 4.16 ± 0.25 pA [no significant difference (t = 1.82)], CV = 28.86 ± 1.0% [no significant difference (t = 1.25)]. Averaged values for 2- to 3-week-old animals: First EPSC, P_r = 0.21 ± 0.03, quantal amplitude = − 3.33 ± 0.15 pA, CV of quantal peak = 30.35 ± 2.82%; second EPSC, P_r = 0.66 ± 0.11 (t = 5.418, $P < 0.005$), quantal amplitude = −3.26 ± 0.2 pA [no significant difference (t = 0.78)], CV = 29.8 ± 1.62% [no significant difference (t = 0.41)]. For all experiments, n = 3.
23. D. Muller, M. Oliver, G. Lynch, *Dev. Brain Res.* **49**, 105 (1989).
24. C. F. Stevens and T. Tsujimoto, *Proc. Natl. Acad. Sci. U.S.A.* **92**, 846 (1995).
25. F. A. Dodge and R. A. Rahamimoff, *J. Physiol. (London)* **193**, 419 (1967); R. A. Mallart and A. R. Martin, *ibid.* **196**, 593 (1968); J. E. Zengel and K. L. Magleby, *J. Gen. Physiol.* **76**, 175 (1980).
26. *N*-Methyl-D-aspartate receptors were blocked with D-2-amino-5-phosphonovaleric acid (50 μM), and the CA1 cell was dialyzed with 10 mM BAPTA [1,2-bis(2-aminophenoxy)ethane-*N,N,N′,N′*-tetraacetic acid] to eliminate changes in CA1 cell internal Ca^{2+} in response to increasing $[Ca^{2+}]_o$. Gaussian fits to quantal peaks were as follows: Fig. 4A, −3.79 ± 1.12 pA; Fig. 4B, −4.0 ± 1.2 pA; Fig. 4C, −4.2 ± 1.32 pA; and Fig. 4D, −4.2 ± 1.3 pA (means ± SD). Averaged values of release parameters for 4- to 8-day-old animals were as follows: Normal $[Ca^{2+}]_o$, P_r = 0.89 ± 0.03, quantal amplitude = −4.14 ± 0.07 pA, CV of quantal peak = 32.8 ± 2.18%, mean EPSC = −3.98 ± 0.16 pA; increased $[Ca^{2+}]_o$, P_r = 0.93 ± 0.02 [no significant difference from value in normal Ca^{2+} (t = 1.19, paired t test)], quantal amplitude = −4.19 ± 0.041 pA [no significant difference (t = 1.64)], CV = 34.1 ± 1.02% [no significant difference (t = 0.53)], mean EPSC = −4.3 ± 0.1 pA [no significant difference (t = 2.42)]. Averaged values for 2- to 3-week-old rats were as follows: Normal $[Ca^{2+}]_o$, P_r = 0.42 ± 0.04, quantal amplitude = −4.4 ± 0.34 pA, CV = 29.96 ± 2.16%, mean EPSC = −1.86 ± 0.4 pA; increased $[Ca^{2+}]_o$, P_r = 0.86 ± 0.02 [significantly different from value in normal Ca^{2+} ($P < 0.005$, paired t test)], quantal amplitude = −4.35 ± 0.19 pA [no significant difference (t = 2.13)], CV = 27.7 ± 1.2% [no significant difference (t = 1.01)], mean EPSC = −3.94 ± 0.24 pA [significant difference ($P < 0.01$)]. For all averages, n = 3.
27. M. Raastad, J. F. Storm, P. Andersen, *Eur. J. Neurosci.* **4**, 113 (1992).
28. C. F. Stevens and Y. Wang, *Neuron* **14**, 795 (1995).
29. K. E. Sorra and K. M. Harris, *J. Neurosci.* **13**, 3736 (1993). A minority of axons appeared to make multiple contacts with a CA1 neuron at the light-microscopic level; in some instances, a single presynaptic bouton contacted two postsynaptic spines.
30. A. J. Gulyas, R. Miles, A. Sik, K. Toth, N. Tamamaka, *Nature* **366**, 683 (1993); O. Arancio, H. Korn, A. Gulyas, T. Freund, R. Miles, *J. Physiol. (London)* **481**, 395 (1994).
31. F. A. Edwards, A. Konnerth, B. Sakmann, *J. Physiol. (London)* **430**, 213 (1990).
32. A. Malgaroli and R. W. Tsien, *Nature* **357**, 134 (1992).
33. C. F. Stevens and Y. Wang, *ibid.* **371**, 704 (1994).
34. A. Malgaroli *et al.*, *Science* **268**, 1624 (1995).
35. T. Manabe, P. Renner, R. A. Nicoll, *Nature* **355**, 50 (1992).
36. D. M. Kullmann and R. A. Nicoll, *ibid.* **357**, 240 (1992); D. Liao, A. Jones, R. Malinow, *Neuron* **9**, 1089 (1992); A. Larkman, T. Hannay, K. Stratford, J. Jack, *Nature* **360**, 70 (1992).
37. S. N. Davies, R. A. J. Lester, K. G. Reymann, G. L. Collingridge, *Nature* **338**, 500 (1989).
38. M. C. Crair and R. C. Malenka, *ibid.* **375**, 325 (1995); A. Kirkwood, H.-K. Lee, M. F. Bear, *ibid.*, p. 328.
39. We thank B. Armitage, R. Hawkins, and E. Kandel for their helpful comments on the manuscript, and R. Malinow for providing computer software for calculation of density estimates.

4 April 1995; accepted 11 July 1995

Regulated Subcellular Distribution of the NR1 Subunit of the NMDA Receptor

Michael D. Ehlers, Whittemore G. Tingley, Richard L. Huganir*

NMDA (*N*-methyl-D-aspartate) receptors are selectively localized at the postsynaptic membrane of excitatory synapses in the mammalian brain. The molecular mechanisms underlying this localization were investigated by expressing the NR1 subunit of the NMDA receptor in fibroblasts. NR1 splice variants containing the first COOH-terminal exon cassette (NR1A and NR1D) were located in discrete, receptor-rich domains associated with the plasma membrane. NR1 splice variants lacking this exon cassette (NR1C and NR1E) were distributed throughout the cell, with large amounts of NR1 protein present in the cell interior. Insertion of this exon cassette into the COOH-terminus of the GluR1 AMPA (α-amino-3-hydroxy-5-methyl-4-isoxazole propionate) receptor was sufficient to cause GluR1 to be localized to discrete, receptor-rich domains. Furthermore, protein kinase C phosphorylation of specific serines within this exon disrupted the receptor-rich domains. These results demonstrate that amino acid sequences contained within the NR1 molecule serve to localize this receptor subunit to discrete membrane domains in a manner that is regulated by alternative splicing and protein phosphorylation.

Aggregation of neurotransmitter receptors in the postsynaptic membrane is a process crucial for synaptogenesis. Like acetylcholine receptors (AChRs) at the neuromuscular junction (*1*), neurotransmitter receptors in the central nervous system (CNS) are localized at postsynaptic sites (*2*–*6*), although the mechanisms involved are less well understood. The NMDA class of glutamate receptors plays a critical role in synaptic plasticity, synaptogenesis, and excitotoxicity (*7*). Iontophoretic mapping and immunoelectron microscopy reveal that NMDA receptors are concentrated at synaptic sites (*4, 5*). Moreover, actin filament stabilization prevents Ca^{2+}-induced rundown of NMDA current (*8*), and NMDA responses are sensitive to cytoskeletal strain (*9*), suggesting a cytoskeletal association of the NMDA receptor.

NMDA receptors consist of two families of homologous subunits (NR1 and NR2A-D) (*10, 11*). The NR1 subunit is able to form functional homomeric channels (*10*), which may be present in vivo (*12, 13*). Expression of NR2 subunits with the NR1 subunit, however, increases NMDA receptor current, and most NMDA receptors in the brain are thought to be heteromeric complexes of NR1 and NR2 subunits (*11, 14*). At least seven NR1 splice variants (NR1A-G) are expressed in the brain (*13, 15, 16*) that differ in their spatial and temporal expression patterns (*17*), in their sensitivity to polyamines, phorbol esters, and Zn^{2+} (*13, 16*), and in their ability to be phosphorylated by protein kinase C (PKC) (*18*).

To examine the mechanism of subcellular targeting of the NR1 subunit, we transfected QT6 quail fibroblasts (*19*) with the complementary DNA (cDNA) encoding the NR1A subunit and examined them by immunofluorescent microscopy (*20, 21*). The QT6 cell line has been used as a model system for studying AChR clustering induced by the synaptic protein 43K (*22*). Immunofluorescent staining revealed the presence of highly concentrated regions of NR1A protein (Fig. 1A). These NR1-enriched domains manifested themselves as patches or elongated stripes as well as punctate microclusters. The organization of NR1 into highly concentrated domains is unique among heterologously expressed glutamate receptors we have examined. For example, the AMPA receptor subunit GluR1 and the kainate receptor subunit GluR6 are found throughout transfected QT6 cells, with large amounts of intracellular staining and no regions of receptor enrichment (Fig. 1, B and C). Indeed, within the same cell cotransfected with both GluR1

Department of Neuroscience, Howard Hughes Medical Institute, Johns Hopkins University School of Medicine, Baltimore, MD 21205, USA.

*To whom correspondence should be addressed.

and NR1 cDNAs, GluR1 protein was found to be distributed throughout the cell (Fig. 1B), whereas NR1 protein was found in discrete NR1-enriched domains (Fig. 1A). Immunoblot analysis of QT6 cell lysates showed that QT6 cells do not express endogenous forms of these receptor subunits and that GluR1, NR1, and GluR6 staining was specific for transfected cells (*23*). The observed receptor-rich domains of NR1 were similar to the clusters of AChRs induced by coexpression of AChR subunits with the synaptic protein 43K (*22*), which suggests that similar mechanisms might be involved in the subcellular localization of these two receptors.

The finding that the NR1 subunit was concentrated in discrete subcellular domains very similar to those reported for 43K-induced AChR clusters suggested that the NR1 molecule contains a region responsible for targeting the receptor subunit to these domains. To determine the region of the NR1 molecule necessary for the formation of the NR1-enriched domains, we expressed four different NR1 splice variants (NR1A, C, D, and E) in fibroblasts and examined their subcellular distribution. The four NR1 splice variants differed only in the presence or absence of two exon cassettes (referred to here as CI and CII) in the COOH-terminal domain of the molecule. Deletion of the 37–amino acid CI exon cassette occurs in-frame, whereas deletion of the 38–amino acid CII exon cassette causes a reading frame shift that results in an altered and slightly truncated COOH-terminal amino acid sequence (*15*). Serines within the CI exon cassette are phosphorylated by PKC (*18*), which suggests that the COOH-terminal region of NR1 is intracellular and could potentially interact with cytoskeletal elements involved in organizing the NR1-enriched domains.

Localization of NR1 protein by immunofluorescent staining showed that the splice variants NR1A and NR1D were concentrated in discrete domains when expressed in QT6 cells, whereas the splice variants NR1C and NR1E were distributed throughout the cell in a manner similar to GluR1 and GluR6 (Fig. 2A). The primary difference between these two pairs of NR1 splice variants is that the CI exon cassette is present in NR1A and NR1D but absent in NR1C and NR1E (Fig. 2A, blue bar). Thus, the 37–amino acid CI exon cassette was necessary for the formation of NR1-enriched domains, which indicates that alternative splicing can regulate the subcellular distribution of the NR1 subunit. Immunoblot analysis of QT6 cell lysates confirmed the specificity of the antibodies and showed that the expression levels of the different splice variants were approximately equal (*23*).

To further examine the effect of the CI cassette on the subcellular distribution of the NR1 subunit, we performed scanning laser confocal microscopy (*24*). Serial 1- to 2-μm optical sections of QT6 cells transfected with either NR1A or NR1C and stained with an NR1 antibody revealed a marked difference in the subcellular location of these two NR1 splice variants. NR1A protein was observed to be associated with the plasma membrane, where it was found in discrete stretches (Fig. 2B). Very little NR1A protein was observed in the interior region of the cell. In contrast, NR1C protein was distributed throughout the entire interior of the cell, excluding the nucleus (Fig. 2B). These findings suggest that the CI cassette, which is present in NR1A but not NR1C, is responsible for the targeting or anchoring of NR1A to structures associated with the plasma membrane, perhaps through a direct interaction with cytoskeletal elements or constituents of the plasma membrane. However, because cell surface labeling experiments have failed to reveal quantitative differences between cell surface NR1A and NR1C, and surface antibody staining has as yet been unsuccessful, we cannot rule out the possibility that the NR1A-enriched domains might lie just beneath the plasma membrane.

The finding that the CI exon cassette was required for localizing the NR1 subunit to plasma membrane–associated NR1-enriched domains, combined with the previous results that serines contained within the CI exon cassette are phosphorylated by PKC (*18*), suggested the possibility that protein phosphorylation might also regulate NR1 distribution. Treatment of NR1A-expressing QT6 cells with the PKC-activating phorbol ester 12-*O*-tetradecanoyl phorbol-13-acetate (TPA) caused rapid disruption of the NR1A-enriched domains, resulting in an altered NR1A subcellular distribution resembling the normal distribution seen for NR1C, GluR1, and

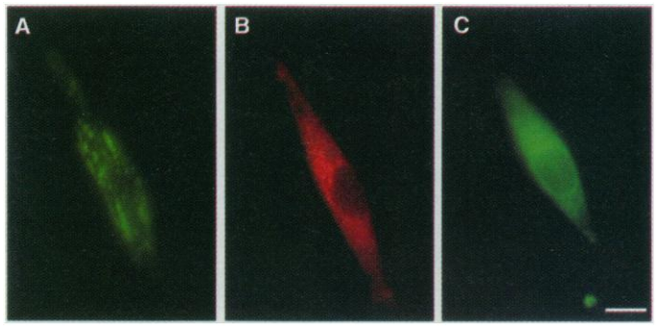

Fig. 1. Expression and distribution of glutamate receptor subunits in fibroblasts. QT6 cells were transiently cotransfected with expression vectors containing NR1 and GluR1 cDNAs (**A** and **B**) or transiently transfected with GluR6 cDNA (**C**) (*20*). Cells were fixed and stained with either antibodies to both NR1 (A) and GluR1 (B) or antibodies to GluR6 (C) and appropriate secondary antibodies conjugated with rhodamine (B) and fluorescein isothiocyanate (FITC) [(A) and (C)] and visualized by immunofluorescent microscopy (*21*). The percentages of transfected cells exhibiting enriched domains of receptor protein were 72 ± 8% for NR1, 0% for GluR1, and 0% for GluR6 (n = 3, >100 cells counted for each experiment). Bar, 10 μm.

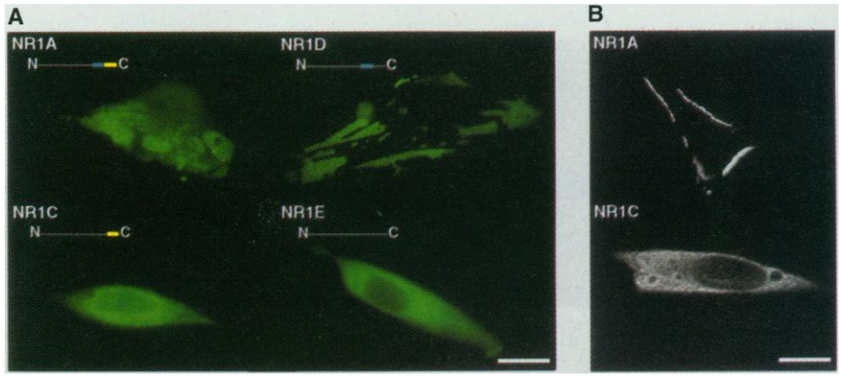

Fig. 2. Regulation of NR1 distribution in fibroblasts by alternative splicing. (**A**) QT6 cells were transiently transfected with the cDNAs for four different NR1 splice variants (NR1A, NR1C, NR1D, and NR1E) that differ in the presence or absence of two exon cassettes (CI and CII) in the COOH-terminal region of the protein [indicated by blue (CI) and yellow (CII) boxed regions] (*20*). Cells were fixed and stained with antibodies to NR1 that recognize COOH-terminal peptide sequences, along with FITC-conjugated secondary antibodies, and visualized by immunofluorescent microscopy (*21*). (**B**) NR1A- and NR1C-expressing QT6 cells were fixed and stained with an NR1 antibody and an FITC-conjugated secondary antibody as in (A), and horizontal optical sections (1 to 2 μm thick) approximately 2 μm above the level of cell attachment were obtained by scanning laser confocal microscopy (*24*). The percentages of transfected cells exhibiting enriched domains of receptor protein were 72 ± 8% for NR1A, 0% for NR1C, 68 ± 8% for NR1D, and 0% for NR1E (n = 3, >100 cells counted for each experiment). Bar, 10 μm.

GluR6 (Fig. 3A, top). Mutation of two serines in the CI exon cassette (S889A and S890A, where S is Ser and A is Ala), which are phosphorylated by PKC (*18*), completely eliminated the phorbol ester–induced disruption of the NR1A-enriched domains (Fig. 3A, middle). However, mutation of two nearby serines in the CI cassette (S896A and S897A), which are also phosphorylated by PKC, had no effect on the phorbol ester–induced disruption of the NR1-enriched domains (Fig. 3A, bottom).

The finding that PKC phosphorylation of different serines located just six residues apart had different effects on the subcellular distribution of NR1 suggests a high degree of specificity in the interaction or interactions responsible for the formation of the receptor-rich domains. Scanning laser confocal microscopy of NR1A-expressing QT6 cells treated with either control solution or phorbol ester showed that TPA treatment induced the rapid redistribution of NR1A protein from discrete, concentrated stretches associated with the plasma membrane to interior regions of the cell (Fig. 3B) (*24*). Again, this altered distribution of NR1A was very similar to the normal distribution of the NR1C subunit observed in QT6 cells. Moreover, the phorbol ester–induced redistribution of NR1A protein was reversible upon washout of the phorbol ester (*25*). Our findings thus indicate that phosphorylation of specific serines contained in the CI exon cassette can regulate the subcellular distribution of the NR1A subunit.

To determine whether the CI cassette was both necessary and sufficient for localizing the NR1 subunit to receptor-enriched domains, we constructed GluR1-NR1 chimeric receptors containing NR1 sequences inserted into the AMPA receptor subunit GluR1 (*26*). The first GluR1-NR1 chimera tested, NGluR1-Cterm, contained the entire NR1 COOH-terminal region from putative transmembrane domain IV to the COOH-terminus (amino acids 834 to 938 of NR1A) inserted into the COOH-terminal region of GluR1 between residues 887 and 888. Wild-type GluR1 protein is normally present throughout transfected QT6 cells, with large amounts of intracellular staining (Fig. 4A). However, transfection of the NGluR1-Cterm cDNA into QT6 cells followed by fixation and immunofluorescent staining with an antibody to GluR1 revealed that the COOH-terminal region of NR1A was sufficient to induce the formation of highly concentrated domains of the NGluR1-Cterm chimeric receptor (Fig. 4B).

To narrow down the region of NR1 sufficient to induce the formation of GluR1-enriched domains, we made a second NR1-GluR1 chimera containing two copies of the CI exon cassette of NR1 (amino acids 859 to 902) inserted in series in the COOH-terminal region of GluR1 between residues 887 and 888 [referred to as NGluR1-$(CI)_2$]. Immunofluorescent staining of QT6 cells expressing the NGluR1-$(CI)_2$ chimera revealed the characteristic concentrated domains of receptor protein observed with NR1A (Fig. 4C). Immunoblot analysis of QT6 cell lysates indicated that the GluR1 antibody specifically recognized wild-type GluR1 and NGluR1 chimeras and that expression levels of the three receptors were approximately equal (*23*). Furthermore, treatment of both NGluR1-Cterm (Fig. 4D) and NGluR1-$(CI)_2$ (Fig. 4E) expressing QT6 cells with phorbol ester resulted in the rapid disruption of the chimeric receptor-rich domains in a manner similar to that of NR1A. These results demonstrated that the CI exon cassette was sufficient to induce GluR1 to form receptor-enriched subcellular domains, which were completely disrupted by treatment with phorbol ester.

NMDA receptors aggregate at synaptic sites (*4*, *5*) and may associate directly or indirectly with the cytoskeleton (*8*, *9*). In addition, neurons in the CNS contain intracellular pools of glutamate receptors, including NMDA receptors (*3*, *4*). In this study, alternative splicing and phosphorylation of the NR1 subunit of the NMDA receptor were shown to regulate the subcellular distribution and plasma membrane association of NR1 subunits expressed in QT6 quail fibroblast cells. Alternative splicing and protein phosphorylation may provide regulatory mechanisms for control of the distribution of the NMDA receptor between intracellular pools and the postsynaptic membrane. Indeed, the temporal pattern of NR1 splice

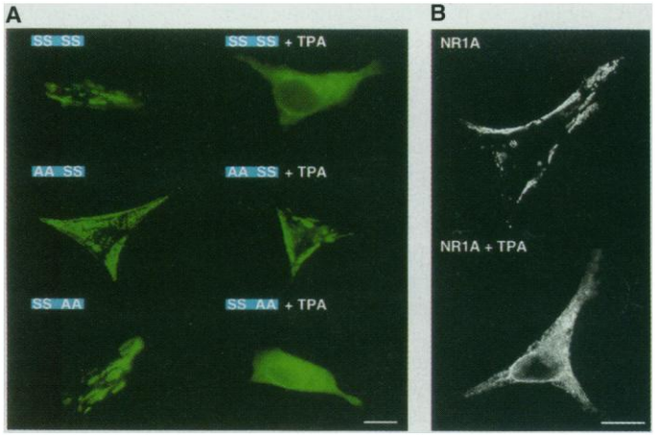

Fig. 3. Regulation of NR1 distribution by protein phosphorylation. (**A**) QT6 cells were transiently transfected with the cDNA for wild-type NR1A (top), an NR1A mutant with Ser (S) at positions 889 and 890 converted to Ala (A) (middle), or an NR1A mutant with Ser at positions 896 and 897 converted to Ala (bottom) (*20*). The cells were treated for 1 hour with either 100 nM TPA (right panels) or control solution (left panels) immediately before fixation and staining with an NR1 antibody and an FITC-conjugated secondary antibody (*21*). Stained cells were then visualized by immunofluorescent microscopy (*21*). Bar, 10 μm. (**B**) NR1A-expressing QT6 cells treated with either 100 nM TPA (bottom) or control solution (top) were fixed and stained with an NR1 antibody and an FITC-conjugated secondary antibody as in (A), and horizontal optical sections (1 to 2 μm thick) approximately 1 μm above the level of cell attachment were obtained by scanning laser confocal microscopy (*24*). Bar, 10 μm.

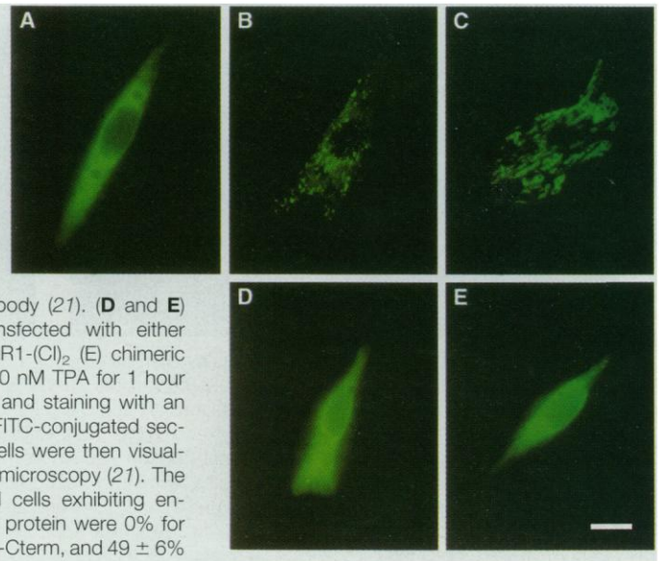

Fig. 4. Identification of NR1 sequences sufficient to induce the formation of GluR1-enriched domains. QT6 cells were transiently transfected with the cDNA for GluR1 (**A**), NGluR1-Cterm (**B**), or NGluR1-$(CI)_2$ (**C**) (*20*), and stained with a GluR1 antibody and an FITC-conjugated secondary antibody (*21*). (**D** and **E**) QT-6 cells transiently transfected with either NGluR1-Cterm (D) or NGluR1-$(CI)_2$ (E) chimeric cDNA were treated with 100 nM TPA for 1 hour immediately before fixation and staining with an antibody to GluR1 and an FITC-conjugated secondary antibody. Stained cells were then visualized by immunofluorescent microscopy (*21*). The percentages of transfected cells exhibiting enriched domains of receptor protein were 0% for GluR1, 27 ± 4% for NGluR1-Cterm, and 49 ± 6% for NGluR1-$(CI)_2$ (n = 3, >100 cells counted for each experiment). Bar, 10 μm.

variant expression appears to be developmentally regulated, with the CI cassette-containing splice variants exhibiting increased expression levels around, and immediately after, the time of birth, a time of intense synaptogenesis in the mammalian CNS (*17*). The role of NR2 subunits in the subcellular localization of NMDA receptors is unknown. The NR2 subunits contain large COOH-terminal domains that are likely to contain additional targeting sequences. Regulation of the cellular distribution, membrane density, and cytoskeletal interactions of NMDA receptors at the synapses may prove to be important processes in both synaptogenesis and in long-term alterations of synaptic efficiency that underlie synaptic plasticity.

REFERENCES AND NOTES

1. S. C. Froehner, *J. Cell Biol.* **114**, 1 (1991); *Annu. Rev. Neurosci.* **16**, 347 (1993).
2. A. M. Craig, C. D. Blackstone, R. L. Huganir, G. Banker, *Neuron* **10**, 1055 (1993).
3. R. S. Petralia and R. J. Wenthold, *J. Comp. Neurol* **318**, 329 (1992); L. J. Martin *et al.*, *Neuroscience* **53**, 327 (1993); N. Eshhar *et al.*, *ibid.* **57**, 943 (1993); G. W. Huntley *et al.*, *J. Neurosci.* **13**, 2965 (1993).
4. R. S. Petralia, N. Yokotani, R. J. Wenthold, *J. Neurosci.* **14**, 667 (1994); G. W. Huntley *et al.*, *ibid.*, p. 3603; R. S. Petralia, Y.-X. Wang, R. J. Wenthold, *ibid.*, p. 6102.
5. K. A. Jones and R. W. Baughman, *Neuron* **7**, 593 (1991).
6. A. Triller *et al.*, *J. Cell Biol.* **101**, 683 (1985).
7. T. V. P. Bliss and G. L. Collingridge, *Nature* **361**, 31 (1993); D. W. Choi and S. M. Rothman, *Annu. Rev. Neurosci.* **13**, 171 (1990); M. Constantine-Paton, H. T. Cline E. Debski, *ibid.*, p. 129.
8. C. Rosenmund and G. L. Westbrook, *Neuron* **10**, 805 (1993).
9. P. Paoletti and P. Ascher, *ibid.* **13**, 645 (1994).
10. K. Moriyoshi *et al.*, *Nature* **354**, 31 (1991).
11. H. Monyer *et al.*, *Science* **256**, 1217 (1992); T. Kutsuwada *et al.*, *Nature* **358**, 36 (1992); H. Meguro *et al.*, *ibid.* **357**, 70 (1992).
12. D. M. Rock and R. L. MacDonald, *Mol. Pharmacol.* **42**, 157 (1992); M. Benveniste and M. L. Mayer, *J. Physiol. (London)* **464**, 131 (1993); L. Zhang *et al.*, *Proc. Natl. Acad. Sci. U.S.A.* **91**, 10883 (1994).
13. G. M. Durand *et al.*, *Proc. Natl. Acad. Sci. U.S.A.* **89**, 9359 (1992).
14. M. Sheng *et al.*, *Nature* **368**, 144 (1994).
15. H. Sugihara *et al.*, *Biochem. Biophys. Res. Commun.* **185**, 826 (1992).
16. M. Hollman *et al.*, *Neuron* **10**, 943 (1993).
17. D. J. Laurie and P. H. Seeburg, *J. Neurosci.* **14**, 3180 (1994).
18. W. G. Tingley, K. W. Roche, A. K. Thompson, R. L. Huganir, *Nature* **364**, 70 (1993); W. G. Tingley and R. L. Huganir, data not shown.
19. C. Moscovici *et al.*, *Cell* **11**, 95 (1977).
20. The cDNAs for NR1A, NR1C, NR1D, NR1E, mutant NR1A S889A S890A, mutant NR1A S896A S897A, GluR1, GluR6, NGluR1-Cterm, and NGluR1-$(CI)_2$, subcloned into an expression vector containing the cytomegalovirus promoter, were transfected into QT6 cells by calcium phosphate coprecipitation with the use of 2 μg of DNA per well in two chambered glass chamber slides (Nunc) or 20 μg per 10-cm culture dish. Approximately 40 to 48 hours after transfection, the cells were processed for immunofluorescent staining or solubilized for immunoblot analysis.
21. The antibodies used in these experiments include affinity-purified guinea pig antibody to GluR1 (1:300 dilution) (*2, 27*), rabbit antibody to GluR6 (1:300 dilution) (*27*), and rabbit antibody to NR1 (1:1000 dilution) (*18*). Additionally, an affinity-purified rabbit antibody to NR1 splice variants lacking the second COOH-terminal exon cassette (CII) was generated against the synthetic peptide KRRAIER-EEGQLQLCSRHRES (where K, Lys; R, Arg; A, Ala; I, Ile; E, Glu; G, Gly; Q, Gln; L, Leu; C, Cys; S, Ser; H, His) corresponding to the COOH-terminus of NR1D and NR1E (1:1000). For immunofluorescent staining, transfected cells were rinsed with phosphate-buffered saline (PBS), fixed with 4% paraformaldehyde in PBS containing 4% sucrose for 15 min at room temperature (RT), permeabilized with 0.25% Triton X-100 in PBS for 5 min at RT, blocked with 10% goat serum in PBS for 1 hour at 37°C, incubated with primary antibody in PBS containing 3% goat serum for 1 hour at RT, incubated with secondary antibody in PBS containing 3% goat serum for 1 hour at RT, and then mounted with use of Vectastain fluorescent mounting media (Vector). Stained cells were visualized with a Zeiss Axiophot fluorescence microscope equipped with rhodamine and fluorescein optics.
22. W. D. Phillips *et al.*, *Science* **251**, 568 (1991); W. D. Phillips *et al.*, *J. Cell Biol.* **123**, 729 (1993); M. M. Maimone and J. P. Merlie, *Neuron* **11**, 53 (1993).
23. Immunoblots were performed as described (*27*) (M. D. Ehlers, W. G. Tingley, R. L. Huganir, data not shown).
24. Optical sections (1 to 2 μm thick) in the *x-y* plane were obtained by scanning laser confocal microscopy with an argon laser and the Bio-Rad MRC-600 confocal microscope system. Excitation was at 488 nm, and emissions were taken between 510 and 515 nm. Images were obtained and processed with COMOS version 6.03 (Bio-Rad).
25. M. D. Ehlers, W. G. Tingley, R. L. Huganir, data not shown.
26. Site-directed mutagenesis was used to introduce a silent mutation in the GluR1 cDNA, converting the third nucleotide from the Ala^{887} codon from a C to a T with the use of the antisense primer 5′-CTCCTC-CGCTAGCTCCTG-3′. This mutation introduced a unique Nhe I restriction site in the COOH-terminal domain of the GluR1 cDNA, which was used as an insertion site for NR1 DNA fragments amplified by the polymerase chain reaction (PCR). The NGluR1-Cterm chimera was generated by insertion of the NR1 DNA fragment obtained by PCR amplification from NR1 cDNA with the sense primer 5′-GATCATGAT-GCTAGCGAGATCGCCTACAAGCGAC-3′ and the antisense primer 5′-CATGATCATGCTAGCGCTC-TCCCTATGACGGGAACACAG-3′, corresponding to amino acids 834 to 938 of NR1 into the introduced Nhe I site of the GluR1 cDNA. The NGluR1-$(CI)_2$ chimera was generated in a similar manner with the sense primer 5′-GATCATGATGCTAGCAGGAA-GAACCTGCAGGATAG-3′ and the antisense primer 5′-CATGATCATGCTAGCGGTGCTCGTGTCTTT GGAGG-3′, corresponding to amino acids 859 to 902 of NR1. Nucleotide sequences of the chimeric receptor constructs were verified by DNA sequencing.
27. C. D. Blackstone *et al.*, *J. Neurochem.* **58**, 1118 (1992); L. A. Raymond, C. D. Blackstone, R. L. Huganir, *Nature* **361**, 637 (1993).

28. The NRI cDNAs were provided by S. Nakanishi and the GluR1 and GluR6 cDNAs by S. Heinemann. This research was supported by the Howard Hughes Medical Institute (R.L.H.) and the Medical Scientist Training Program (M.D.E. and W.G.T.). Special thanks go to C. L. Pinch for assisting in the preparation of the manuscript.

10 February 1995; accepted 18 August 1995

Domain Interaction Between NMDA Receptor Subunits and the Postsynaptic Density Protein PSD-95

Hans-Christian Kornau, Leslie T. Schenker, Mary B. Kennedy, Peter H. Seeburg*

The *N*-methyl-D-aspartate (NMDA) receptor subserves synaptic glutamate-induced transmission and plasticity in central neurons. The yeast two-hybrid system was used to show that the cytoplasmic tails of NMDA receptor subunits interact with a prominent postsynaptic density protein PSD-95. The second PDZ domain in PSD-95 binds to the seven–amino acid, COOH-terminal domain containing the terminal *t*SXV motif (where S is serine, X is any amino acid, and V is valine) common to NR2 subunits and certain NR1 splice forms. Transcripts encoding PSD-95 are expressed in a pattern similar to that of NMDA receptors, and the NR2B subunit co-localizes with PSD-95 in cultured rat hippocampal neurons. The interaction of these proteins may affect the plasticity of excitatory synapses.

NMDA receptors comprise a family of ionotropic glutamate receptors (*1*) with properties that indicate they have a central role in synaptic plasticity and memory formation (*2*). These receptors are formed by assembly of the principal subunit NR1 (*3*) with different modulatory NR2 subunits (NR2A-D) (*4*). A conspicuous structural feature of the NR2 subunits is their extended, intracellular COOH-terminal sequence distal to the last transmembrane region (*5*), which may anchor the receptors or assemble a signal-transducing complex for the voltage-dependent Ca^{2+} entry through the glutamate-activated ion channel (*6*). Thus, we set out to identify intracellular proteins that bind to the NR2 subunits at synapses.

We used the two-hybrid system (*7*) to identify such cellular targets for the COOH-terminal domain of NR2 subunits. A bait consisting of the yeast *GAL4* DNA binding domain (amino acids 1 to 147) fused to the entire COOH-terminal domain (627 amino

H.-C. Kornau and P. H. Seeburg, Center for Molecular Biology (ZMBH), University of Heidelberg, INF 282, 69120 Heidelberg, Germany.
L. T. Schenker and M. B. Kennedy, Division of Biology, California Institute of Technology, Pasadena, CA 91125, USA.

*To whom correspondence should be addressed.